

Role of Hec1 in Spindle Checkpoint Signaling and Kinetochores Recruitment of Mad1/Mad2

Silvia Martin-Lluesma, Volker M. Stucke, Erich A. Nigg*

The spindle checkpoint delays sister chromatid separation until all chromosomes have undergone bipolar spindle attachment. Checkpoint failure may result in chromosome mis-segregation and may contribute to tumorigenesis. We showed that the human protein Hec1 was required for the recruitment of Mps1 kinase and Mad1/Mad2 complexes to kinetochores. Depletion of Hec1 impaired chromosome congression and caused persistent activation of the spindle checkpoint, indicating that high steady-state levels of Mad1/Mad2 complexes at kinetochores were not essential for checkpoint signaling. Simultaneous depletion of Hec1 and Mad2 caused catastrophic mitotic exit, making Hec1 an attractive target for the selective elimination of spindle checkpoint-deficient cells.

The genomic stability of all organisms depends on the correct segregation of chromosomes during cell division (1, 2). The accuracy of this process is monitored by the spindle assembly checkpoint (3, 4). This surveillance mechanism is able to detect a single unaligned chromosome, causing a prometaphase arrest until proper bipolar attachment is achieved (5). First identified in yeast, several core checkpoint components have also been characterized in multicellular organisms (6–9). In humans, these include the protein kinases Bub1, BubR1, Mps1, the Bub1/R1-partner Bub3 (10, 11), and the Mad1/Mad2 complex (12, 13). All these proteins localize to kinetochores, particularly during early stages of mitosis (3). The prevailing model of spindle checkpoint function holds that the absence of an appropriate kinetochore-microtubule (MT) interaction generates a signal that inhibits the activity of a ubiquitin ligase termed anaphase-promoting complex/cyclosome (APC/C). In turn, APC/C activates the proteolytic degradation of securin, an inhibitor of sister chromatid separation (2). Both Mad2 (14–16) and multiprotein complexes comprising Mad2, BubR1, and Bub3 (17, 18) have been implicated in the inhibition of APC/C. Upon proper attachment of the last kinetochore, the APC/C-inhibitory signal is extinguished, and anaphase ensues.

At the heart of this model, two key questions need to be answered. First, how is a cell cycle-inhibitory signal generated at unattached kinetochores, and second, how is this signal extinguished upon attachment of the

last kinetochore? Early models for the generation of an inhibitory signal have emphasized the importance of a transient association of a Mad1/Mad2 complex with unattached kinetochores. Conversely, the loss of Mad2 from kinetochores has been correlated with checkpoint silencing (4, 19). However, the kinetochore association of checkpoint components may depend on whether tension and/or MT attachment is impaired at the kinetochore (3, 20, 21). Furthermore, soluble APC/C-inhibitory complexes exist already in interphase cells before kinetochore assembly (17).

In a yeast two-hybrid screen for human Mad1-interacting proteins (22), we isolated a cDNA coding for full-length human Hec1 (highly expressed in cancer) (23) (fig. S1A). This coiled-coil protein is a putative mammalian homolog of budding yeast Ndc80p (24). The exact functions of Hec1 and Ndc80p are unknown, but both proteins localize to kinetochores (23, 25). Yeast Ndc80p forms a complex with kinetochore proteins Nuf2p, Spc24p, and Spc25p, and mutational inactivation of these components causes defects in chromosome segregation (25–27). Similarly, microinjection of antibodies to Hec1 into mammalian cells disrupts mitotic progression (23). As shown by immunofluorescence microscopy, Hec1 was present on kinetochores throughout mitosis (fig. S1B) (23, 25), whereas Mad1 was released upon alignment of chromosomes at the metaphase plate (fig. S1B) (28). Mapping of the Hec1 and Mad2 binding sites on Mad1 revealed them to be distinct, indicating that Mad1 could bind both proteins simultaneously (fig. S1A).

To directly explore the functional significance of the Hec1–Mad1 interaction in HeLa S3 cells, gene silencing by small interfering RNA (siRNA) was used (29). Immunofluorescence microscopy (Fig. 1A and fig. S2)

tated by concentrating motors into lipid raft domains (13) or by enhancing neck coiled-coil stability, possibly by factors binding to the FHA domain located adjacent to the Unc104/KIF1A neck coiled-coil (fig. S3).

References and Notes

1. A. J. Otsuka *et al.*, *Neuron* **6**, 113 (1991).
2. Y. Okada, H. Yamazaki, Y. Sekine-Aizawa, N. Hirokawa, *Cell* **81**, 769 (1995).
3. H. M. Zhou, I. Brust-Mascher, J. M. Scholey, *J. Neurosci.* **21**, 3749 (2001).
4. R. D. Vale, R. A. Milligan, *Science* **288**, 88 (2000).
5. D. W. Pierce, N. Horn-Booher, A. J. Otsuka, R. D. Vale, *Biochemistry* **38**, 5412 (1999).
6. Y. Okada, N. Hirokawa, *Science* **283**, 1152 (1999).
7. ———, *Proc. Natl. Acad. Sci. U.S.A.* **97**, 640 (2000).
8. M. Kikkawa, Y. Okada, N. Hirokawa, *Cell* **100**, 241 (2000).
9. M. Kikkawa *et al.*, *Nature* **411**, 439 (2001).
10. In our assays, neither the dimeric Unc104 motors nor the truncated monomers (U362-GFP or U371-GFP) displayed the biased diffusional motion reported by Okada and Hirokawa (6, 7). However, we were able to observe this motion only by adding extra positively charged residues to the neck linker region and under specific buffer condition (see movie S6 legend for details).
11. R. D. Vale, R. J. Fletterick, *Annu. Rev. Cell Dev. Biol.* **13**, 745 (1997).
12. G. S. Bloom, *Curr. Opin. Cell Biol.* **13**, 36 (2001).
13. D. R. Klopfenstein, M. Tomishige, N. Stuurman, R. D. Vale, *Cell* **109**, 347 (2002).
14. Materials and methods are available as supporting material on Science Online.
15. K. R. Rogers *et al.*, *EMBO J.* **20**, 5101 (2001).
16. To achieve motility velocities of 2 $\mu\text{m/s}$ with an 8-nm step size, one would predict an adenosine triphosphatase catalytic rate constant of ~ 125 adenosine 5'-triphosphate (ATP)/s per head for the constitutive Unc104 dimers. Our measured rates varied depending on the protein preparation but were in the range of 30 to 100 ATP/s per head, suggesting that some portion of the molecules may be inactive. The microtubule concentration for half-maximal ATPase stimulation of U356-Kstalk-GFP (0.078 μM) was two orders of magnitude smaller than that of U653 (5), indicating an increased microtubule affinity.
17. K. Svoboda, S. M. Block, *Cell* **77**, 773 (1994).
18. The I362E/L365K mutation is predicted to decrease the probability of coiled-coil formation in Unc104's neck coiled-coil from 0.22 to 0.002 (using the computer program COILS version 2.2) but not to change probabilities of the other two coiled-coils (405 to 451 and 595 to 651 amino acids). The chemical cross-linking experiment (14) showed that U403-Kstalk2-GFP containing the I362E/L365K mutation was still a dimer (22).
19. KIF1C, a member of the Unc104/KIF1 subfamily, has been shown to dimerize in fibroblasts overexpressing KIF1C, but not under physiological conditions (23).
20. K. S. Thorn, J. A. Ubersax, R. D. Vale, *J. Cell Biol.* **151**, 1093 (2000).
21. M. Tomishige, R. D. Vale, *J. Cell Biol.* **151**, 1081 (2000).
22. Data not shown.
23. C. Dörner, A. Ullrich, H.-U. Haring, R. Lammers, *J. Biol. Chem.* **274**, 33654 (1999).
24. We thank U. Wiedemann for support in cloning, N. Stuurman and Y. Cui for helpful discussions, and B. Schnapp for providing rat KIF1A cDNA. Supported by grants from the Howard Hughes Medical Institute and NIH (grant AR42895).

Supporting Online Material

www.sciencemag.org/cgi/content/full/297/5590/2263/DC1

Materials and Methods

Figs. S1 to S3

Table S1

References

Movies S1 to S6

29 April 2002; accepted 8 August 2002

Department of Cell Biology, Max-Planck-Institute of Biochemistry, Am Klopferspitz 18a, D-82152 Martinsried, Germany.

*To whom correspondence should be addressed. E-mail: nigg@biochem.mpg.de

REPORTS

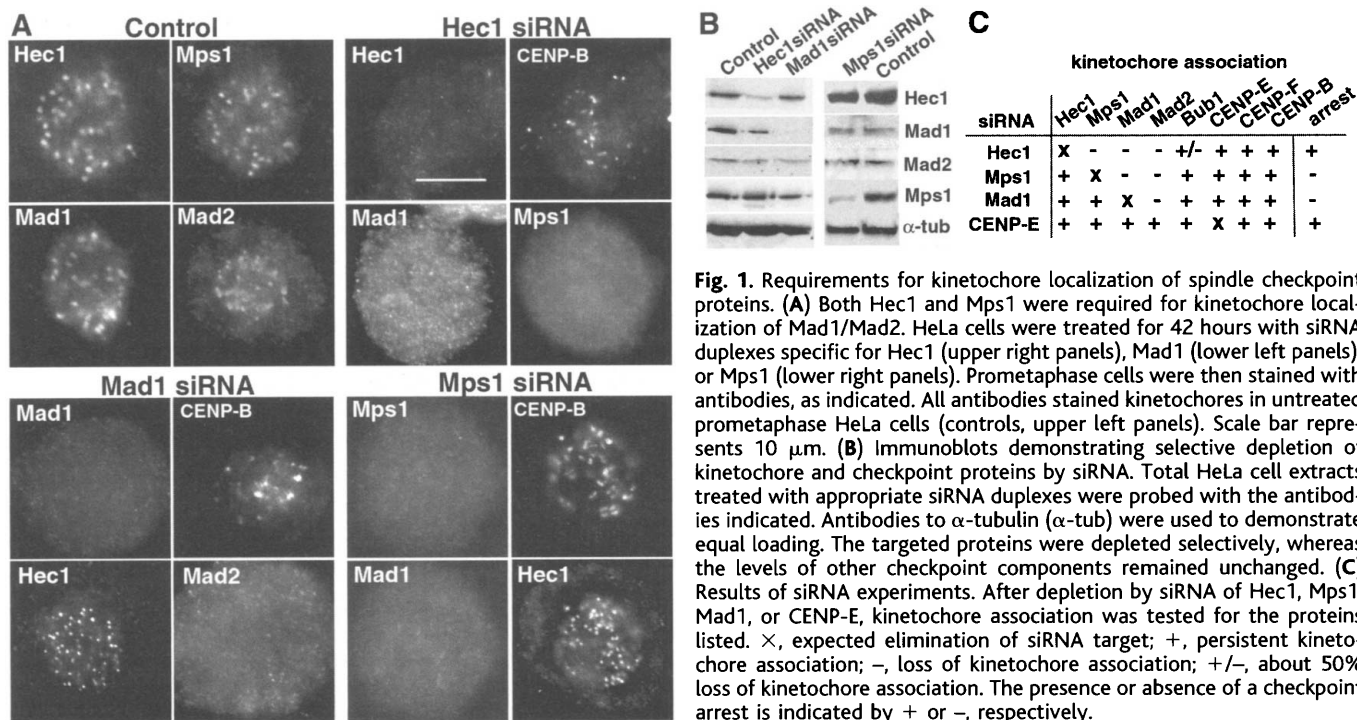


Fig. 1. Requirements for kinetochore localization of spindle checkpoint proteins. (A) Both Hec1 and Mps1 were required for kinetochore localization of Mad1/Mad2. HeLa cells were treated for 42 hours with siRNA duplexes specific for Hec1 (upper right panels), Mad1 (lower left panels), or Mps1 (lower right panels). Prometaphase cells were then stained with antibodies, as indicated. All antibodies stained kinetochores in untreated prometaphase HeLa cells (controls, upper left panels). Scale bar represents 10 μ m. (B) Immunoblots demonstrating selective depletion of kinetochore and checkpoint proteins by siRNA. Total HeLa cell extracts treated with appropriate siRNA duplexes were probed with the antibodies indicated. Antibodies to α -tubulin (α -tub) were used to demonstrate equal loading. The targeted proteins were depleted selectively, whereas the levels of other checkpoint components remained unchanged. (C) Results of siRNA experiments. After depletion by siRNA of Hec1, Mps1, Mad1, or CENP-E, kinetochore association was tested for the proteins listed. X, expected elimination of siRNA target; +, persistent kinetochore association; -, loss of kinetochore association; +/-, about 50% loss of kinetochore association. The presence or absence of a checkpoint arrest is indicated by + or -, respectively.

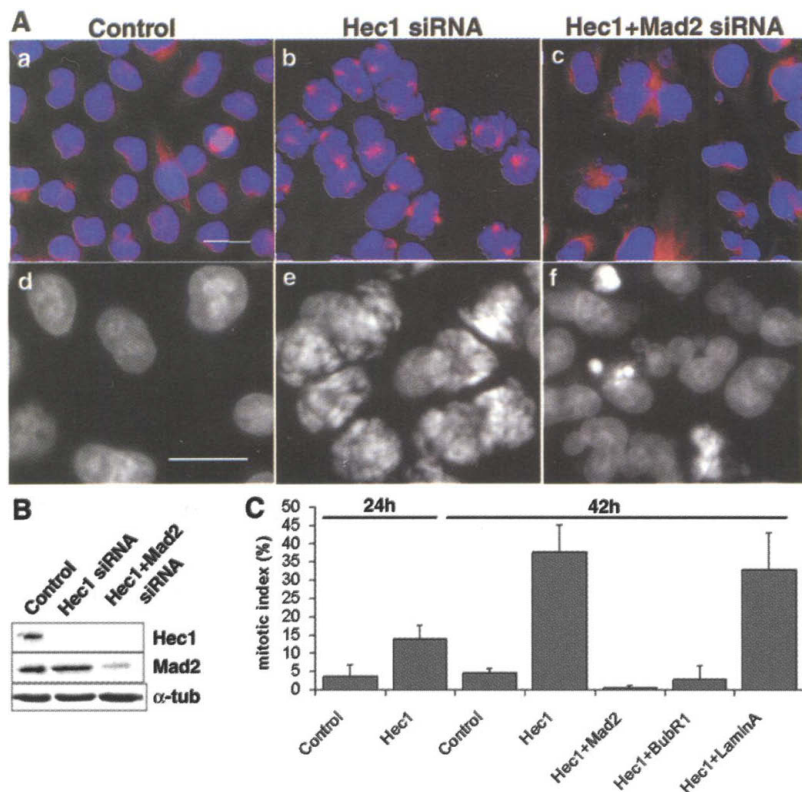


Fig. 2. Depletion of Hec1 caused spindle checkpoint-mediated prometaphase arrest. (A) HeLa cells were treated for 42 hours with siRNA duplexes as indicated and stained with 4',6'-diamidino-2-phenylindole (DAPI, blue) and antibodies to α -tubulin (red). Top row, merged colors; bottom row, enlarged views illustrating DNA condensation states. For illustrative purposes, (b) and (e) show fields with above-average percentages of arrested cells. Scale bars represent 20 μ m. (B) Immunoblot demonstrating depletion of Hec1 and Mad2. Total HeLa cell extracts treated with appropriate siRNA duplexes were probed with the antibodies indicated. Antibodies to α -tubulin were used to demonstrate equal loading. (C) Mitotic indices of HeLa cells treated for 24 or 42 hours with siRNA duplexes depleting the indicated proteins. Histograms show average results and standard deviations from several independent experiments, counting at least 100 cells in at least three different fields in each experiment.

and immunoblotting (Fig. 1B) demonstrated efficient and uniform Hec1 depletion (22). In the absence of Hec1, neither Mad1 nor Mad2 (30) could be detected on kinetochores, although strong kinetochore staining was seen in control cells (Fig. 1A). In contrast, depletion of Mad1 by siRNA did not interfere with Hec1 localization, although it abolished the kinetochore association of Mad2 (Fig. 1A). Thus, the recruitment of the Mad1/Mad2 complex to kinetochores depended on Hec1 but not vice versa. Hec1-depleted cells were also stained with antibodies against Mps1, Bub1, and the centromere proteins CENP-B, CENP-E, or CENP-F. The kinetochore association of Mps1 was completely abolished and that of Bub1 was reduced by about 50%, whereas CENP-B, -E, and -F still localized to kinetochores efficiently (Fig. 1, A and C). Thus, the elimination of Hec1 interfered with the kinetochore association of a specific subset of checkpoint proteins.

We have not been able to reconstitute direct binding between recombinant Hec1 and Mad1 proteins (30), which suggests that additional components are required for this interaction in vivo. We focused on Mps1, as this kinase is required for kinetochore recruitment of the Mad1/Mad2 complex in *Xenopus* egg extracts (31). The siRNA-mediated depletion of human Mps1 abolished the kinetochore association of Mad1 but not of CENP-B or Hec1 (Fig. 1A). Thus, Hec1 was required for the kinetochore association of Mps1, and both Hec1 and Mps1 were required for recruiting the Mad1/Mad2 complex. No binding could be observed between

REPORTS

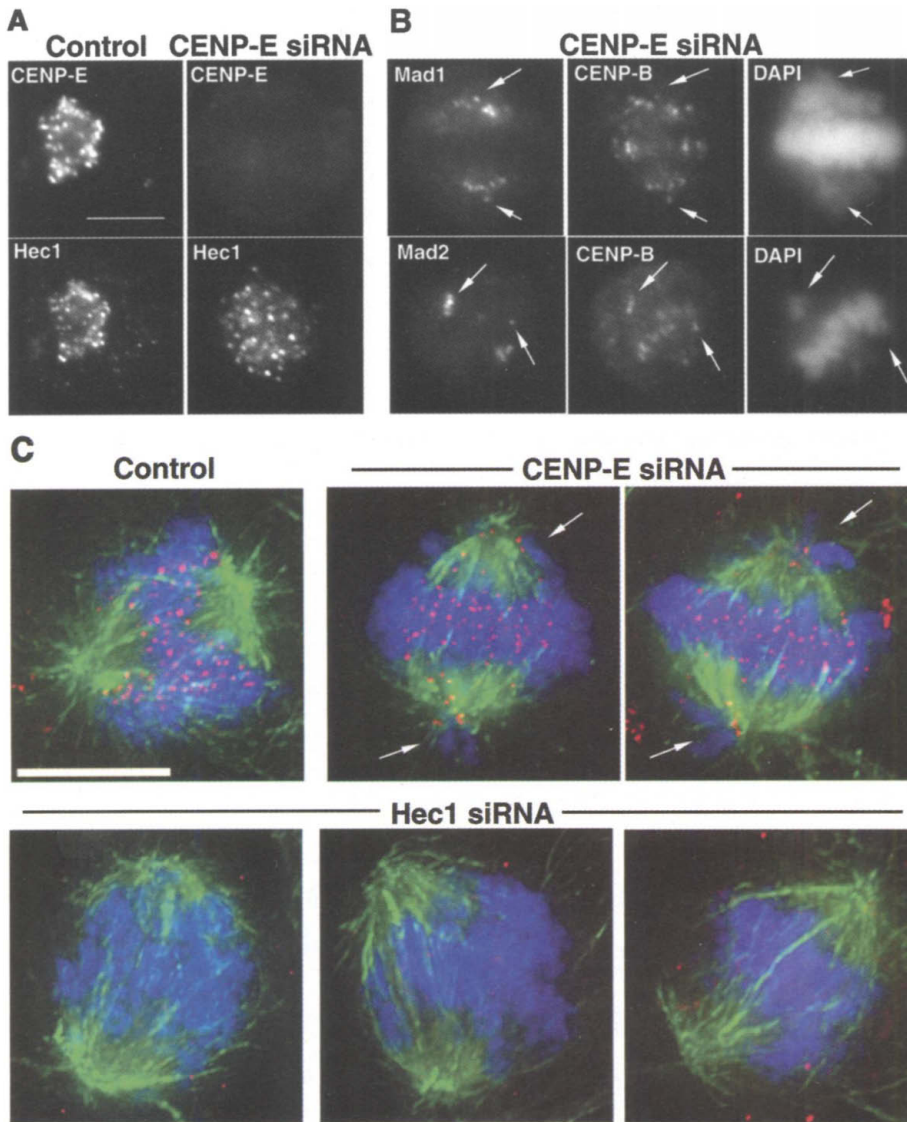


Fig. 3. CENP-E siRNA produced spindle checkpoint arrest with Hec1 and Mad1/Mad2 on kinetochores. (A) Mitotic HeLa cells treated with or without an siRNA duplex specific for CENP-E were double-stained with antibodies to CENP-E (top row) and to Hec1 (bottom row). (B) CENP-E-depleted mitotic HeLa cells were double-stained with antibodies to CENP-B and to either Mad1 or Mad2. DNA staining shows the typical arrest phenotype of CENP-E-depleted cells, with most chromosomes aligned at the metaphase plate and a few trailing, misaligned chromosomes (arrows). The kinetochores of unaligned chromosomes were positive for both Mad1 and Mad2. (C) Comparison of mitotic arrest phenotypes produced by depletion of CENP-E (top row) and Hec1 (bottom row). After siRNA treatment, cells were stained with DAPI (blue) and with antibodies to α -tubulin (green) and to Hec1 (red). Partial formation of metaphase plates occurs in the presence of lagging chromosomes (arrows) in the CENP-E siRNA-treated cells, but prometaphase-like chromosome configurations appear in Hec1 siRNA-treated cells (see also fig. S4). The control shows a typical early metaphase cell. Scale bars represent 10 μ m.

Mps1 and Hec1 in a yeast two-hybrid assay (32), suggesting that in vivo interactions between Hec1, Mps1, and Mad1 require additional components or modifications.

Cultures subjected to Hec1 siRNA treatment displayed a high percentage of cells with condensed chromosomes, suggesting a prometaphase arrest (Fig. 2A, b and e, and Fig. 2C). Chromosomes were almost certainly attached to the spindles, as suggested by the observations that kinetochore MTs

selectively resisted short calcium treatment (33) and kinetochores stained positively for the MT plus end-binding protein EB1 (30). However, virtually none of the chromosomes were aligned in a metaphase plate, which indicates an underlying defect in chromosome congression (Fig. 3C and fig. S3). To examine whether this phenotype was dependent on a functional spindle checkpoint, cells were subjected to siRNA for both Hec1 and Mad2. Upon simulta-

neous depletion of both proteins (Fig. 2B), the accumulation of mitotic cells was abolished (Fig. 2A, c and f, and C). Instead, cells apparently passed through mitosis (Fig. 2C and fig. S4), giving rise to severe nuclear aberrations, including multinucleation and nuclear fragmentation (Fig. 2A, c and f). A similar reduction in the mitotic index was seen after simultaneous depletion of Hec1 and BubR1, another component of the spindle checkpoint, but co-depletion of the lamin A protein was without effect (Fig. 2C). Thus, depletion of Hec1 resulted in persistent activation of the spindle checkpoint and in mitotic catastrophe if the checkpoint was impaired.

The phenotype of Hec1-depleted cells suggested a role for Hec1 in MT-kinetochore interactions, consistent with data obtained for budding yeast Ndc80p (26). In vertebrate cells, a key role in MT-kinetochore interactions has previously been attributed to the kinesin-related motor protein CENP-E (34). Therefore, we examined the consequences of depleting CENP-E. After 42 hours of siRNA treatment, CENP-E could no longer be detected at kinetochores, but Hec1 was still present (Fig. 3A). Moreover, about 20 to 25% of cells displayed a mitotic checkpoint arrest (34, 35) that was abolished upon concurrent elimination of either Mad2 or BubR1 (30). Although the phenotypes observed in response to depletion of Hec1 and CENP-E were superficially similar, they differed in two important aspects. First, chromosome congression to a metaphase plate occurred to a greater extent in cells lacking CENP-E than in cells lacking Hec1 (Fig. 2Ae; Fig. 3, B and C; and fig. S3), consistent with earlier studies on CENP-E (36). Second, chromosomes already aligned at the metaphase plate in CENP-E-depleted cells showed neither Mad1 nor Mad2 on kinetochores, but the kinetochores of unattached chromosomes stained positively for both proteins (Fig. 3B, arrows). In contrast, Hec1-depleted cells displayed a checkpoint arrest although neither Mad1 nor Mad2 could be detected at any kinetochores. Thus, whereas the localization of the Mad1/Mad2 complex in CENP-E-depleted cells was in agreement with the prevailing paradigm for checkpoint signaling, this was not the case in Hec1-depleted cells. Although the spindle checkpoint was active in Hec1-depleted cells, there was no evidence for Mad1/Mad2 association with kinetochores at any time during mitosis. Considering the short half-life of Mad2 at kinetochores (19), it is possible that undetectably low levels of kinetochore-associated Mad1/Mad2 complexes are sufficient for checkpoint signaling. Alternatively, a factor whose kinetochore association does not de-

REPORTS

pend on Hec1 may signal checkpoint activation through diffusible Mad2 complexes. In Hec1-depleted cells, this activity could be generated through CENP-E or BubR1. Because kinetochores were not stretched in Hec1-depleted cells (30), it is plausible that persistent checkpoint activity was caused by lack of tension.

Injection of antibodies to Hec1 into bladder carcinoma cells was reported to cause aberrant mitotic progression and cell death but no checkpoint arrest (23). This result could be explained if these tumor cells were checkpoint-deficient or if the injected antibodies interfered with checkpoint signaling. In *Saccharomyces cerevisiae*, mutations in the Hec1 homolog *Ndc80* caused chromosome segregation defects without activating the checkpoint (24, 26). This may relate to the fact that kinetochores in budding yeast bind only a single MT, whereas those in vertebrate cells capture multiple MTs (8, 9). Furthermore, kinetochore-MT interactions and checkpoint signaling in vertebrates may involve two distinct pathways: one centered on Hec1 interacting with Mad1/Mad2 and the other on CENP-E interacting with CENP-F and BubR1, both pathways converging onto APC/C (35, 36). Yeast has a clear counterpart of Hec1 but lacks an obvious homolog of CENP-E.

The human kinetochore protein Hec1 was required, together with Mps1, for recruiting the Mad1/Mad2 complex to kinetochores. Moreover, Hec1-depleted cells displayed persistent spindle checkpoint activity although they lacked significant amounts of Mad1 or Mad2 at kinetochores. This latter observation contrasts with models emphasizing the importance of high steady-state levels of kinetochore-associated Mad1/Mad2 complexes in checkpoint signaling and instead suggests that some protein that does not depend on Hec1 for kinetochore localization is able to communicate with diffusible Mad2 complexes. Many tumor cells are thought to be defective in the spindle checkpoint (37). Any interference with Hec1 function in checkpoint-deficient cells, be it through siRNA or other specific inhibitors, is predicted to result in mitotic catastrophe, thereby causing the demise of most progeny. In contrast, normal checkpoint-proficient cells may arrest transiently in response to reversible Hec1 inhibition. Thus, Hec1 may be an attractive target for therapeutic intervention in cancer and other hyperproliferative diseases.

References and Notes

1. R. B. Nicklas, *Science* **275**, 632 (1997).
2. K. Nasmyth, J. M. Peters, F. Uhlmann, *Science* **288**, 1379 (2000).

3. A. Musacchio, K. Hardwick, *Nature Rev. Mol. Cell Biol.*, in press.
4. J. V. Shah, D. W. Cleveland, *Cell* **103**, 997 (2000).
5. C. L. Rieder, R. W. Cole, A. Khodjakov, G. Sluder, *J. Cell Biol.* **130**, 941 (1995).
6. M. A. Hoyt, L. Totis, B. T. Roberts, *Cell* **66**, 507 (1991).
7. R. Li, A. W. Murray, *Cell* **66**, 519 (1991).
8. K. Kitagawa, P. Hieter, *Nature Rev. Mol. Cell Biol.* **2**, 678 (2001).
9. C. L. Rieder, E. D. Salmon, *Trends Cell Biol.* **8**, 310 (1998).
10. V. M. Stucke, H. H. Sillje, L. Arnaud, E. A. Nigg, *EMBO J.* **21**, 1723 (2002).
11. S. S. Taylor, E. Ha, F. McKeon, *J. Cell Biol.* **142**, 1 (1998).
12. X. Luo, Z. Tang, J. Rizo, H. Yu, *Mol. Cell* **9**, 59 (2002).
13. L. Sironi et al., *EMBO J.* **20**, 6371 (2001).
14. G. Fang, H. Yu, M. W. Kirschner, *Genes Dev.* **12**, 1871 (1998).
15. M. Kallio, J. Weinstein, J. R. Daum, D. J. Burke, G. J. Gorbosky, *J. Cell Biol.* **141**, 1393 (1998).
16. L. H. Hwang et al., *Science* **279**, 1041 (1998).
17. V. Sudakin, G. K. Chan, T. J. Yen, *J. Cell Biol.* **154**, 925 (2001).
18. Z. Tang, R. Bharadwaj, B. Li, H. Yu, *Dev. Cell* **1**, 227 (2001).
19. B. J. Howell, D. B. Hoffman, G. Fang, A. W. Murray, E. D. Salmon, *J. Cell Biol.* **150**, 1233 (2000).
20. D. A. Skoufias, P. R. Andreassen, F. B. Lacroix, L. Wilson, R. L. Margolis, *Proc. Natl. Acad. Sci. U.S.A.* **98**, 4492 (2001).
21. J. C. Waters, R. H. Chen, A. W. Murray, E. D. Salmon, *J. Cell Biol.* **141**, 1181 (1998).
22. Materials and methods are available as supporting material on Science Online.
23. Y. Chen, D. J. Riley, P. L. Chen, W. H. Lee, *Mol. Cell Biol.* **17**, 6049 (1997).
24. P. A. Wigge et al., *J. Cell Biol.* **141**, 967 (1998).
25. P. A. Wigge, J. V. Kilmartin, *J. Cell Biol.* **152**, 349 (2001).
26. X. He, D. R. Rines, C. W. Espelin, P. K. Sorger, *Cell* **106**, 195 (2001).
27. C. Janke et al., *EMBO J.* **20**, 777 (2001).
28. M. S. Campbell, G. K. T. Chan, T. J. Yen, *J. Cell Sci.* **114**, 953 (2001).
29. S. M. Elbashir et al., *Nature* **411**, 494 (2001).
30. S. Martin-Lluesma, E. A. Nigg, unpublished observations.
31. A. Abrieu et al., *Cell* **106**, 83 (2001).
32. V. M. Stucke, E. A. Nigg, unpublished observations.
33. T. M. Kapoor, T. U. Mayer, M. L. Coughlin, T. J. Mitchison, *J. Cell Biol.* **150**, 975 (2000).
34. X. B. Yao, A. Abrieu, Y. Zheng, K. F. Sullivan, D. W. Cleveland, *Nature Cell Biol.* **2**, 484 (2000).
35. G. K. Chan, S. A. Jablonski, V. Sudakin, J. C. Hittle, T. J. Yen, *J. Cell Biol.* **146**, 941 (1999).
36. B. F. McEwen et al., *Mol. Biol. Cell* **12**, 2776 (2001).
37. C. Lengauer, K. W. Kinzler, B. Vogelstein, *Nature* **396**, 643 (1998).
38. We thank D. Brown, W. Earnshaw, J. Kilmartin, and T. U. Mayer for antibodies; F. Barr, S. Elledge, and K. T. Jeang for plasmids; F. Barr for advice on yeast work; and all members of the laboratory for helpful discussions.

Supporting Online Material

www.sciencemag.org/cgi/content/full/297/5590/2267/DC1

Materials and Methods

Figs. S1 to S4

References and Notes

1 July 2001; accepted 13 August 2002

Gene Expression During the Life Cycle of *Drosophila melanogaster*

Michelle N. Arbeitman,^{1*} Eileen E. M. Furlong,^{2,3,5} Farhad Imam,^{3,4*} Eric Johnson,^{3,4,6*} Brian H. Null,^{2,7*} Bruce S. Baker,¹ Mark A. Krasnow,^{3,4} Matthew P. Scott,^{2,4} Ronald W. Davis,^{3,7} Kevin P. White^{7,8†}

Molecular genetic studies of *Drosophila melanogaster* have led to profound advances in understanding the regulation of development. Here we report gene expression patterns for nearly one-third of all *Drosophila* genes during a complete time course of development. Mutations that eliminate eye or germline tissue were used to further analyze tissue-specific gene expression programs. These studies define major characteristics of the transcriptional programs that underlie the life cycle, compare development in males and females, and show that large-scale gene expression data collected from whole animals can be used to identify genes expressed in particular tissues and organs or genes involved in specific biological and biochemical processes.

Molecular studies of development in multicellular organisms have gone through two major phases during the past three decades. Initially, solution hybridization studies quantitated transcript abundance and showed that large-scale changes in gene expression accompany development (1). In *Drosophila*, such studies suggested that 5000 to 7000 different polyadenylated RNA species are produced at each stage of the life cycle and

that the composition of this set of RNAs shifted during development (1). These analyses gave an overview of genome activity during development, but they could not follow the expression of individual genes or reveal their identities. Later, when it became possible to clone individual genes (2, 3), RNA blots and in situ hybridization revealed when and where individual genes were active. This second phase of analysis allowed